Experimental und numerical investigations of ductile failure behavior in the ferritic steel

Pawel Kucharczyk[1*], Sebastian Münstermann[1]

[1] Department of Ferrous Metallurgy, RWTH Aachen University, Intzestr. 1, 52056 Aachen, Germany

[*] pawel.kucharczyk@iehk.rwth-aachen.de

Keywords: ductile damage and failure behavior, crack initiation, damage mechanics model, FEM simulation.

Abstract

In the process of the ductile failure of steels three phases can be distinguished: voids nucleation, growth, and their coalescence leading to the initiation of a micro-crack. The initiation and the further propagation of the micro-crack are mainly influenced by the amount, size and distribution of inclusions or precipitations as well as by imperfections of the lattice structure. The ductile failure is accompanied by large plastic deformation and significant strain gradients in the loaded material. Therefore, for the numerical simulation of ductile damage mechanisms a precise description of the material plasticity and an exact definition of the failure criterion are required. In the recent years many different damage mechanics models have been developed, which can be basically classified into coupled and uncoupled models. The models of the first group consider the effect of the accumulated damage in the form of the constitutive equations. For the uncoupled models a critical loading condition responsible for the appearance of fracture has to be defined.

In the frames of this work a coupled damage mechanics model has been derived from the combination of different types of damage approaches and utilized for the numerical simulation of the ductile failure behavior. The main feature of the applied model is that it considers the influence of stress triaxiality, defined as the ratio of pressure over the equivalent stress, and of the Lode angle, related to the third invariant of the deviatoric stress tensor, on the hardening behavior. Furthermore, a new definition of the onset and the progress of damage in the material has been introduced. In order to indicate, when the damage starts to play a role in the failure process, the micro-crack initiation was estimated using the direct current potential drop (DCPD) method. Further numerical simulation allowed for the determination of the crack initiation locus. The consecutive microstructure degradation was described using a dissipation-energy-based damage evolution law. This approach was implemented into ABAQUS/Explicit by means of a user's material subroutine (VUMAT).

The ductile failure behavior was experimentally and numerically investigated in the ferritic steel 22NiMoCr3-7. The procedure used for the calibration of the material parameters and for the estimation of the crack initiation locus is presented.

Introduction

In the design of constructions the ductile failure behavior is preferable to brittle failure behavior due to significant plastic deformation before the final fracture. The mechanism of this failure type is well known and comprises the voids nucleation, their growth to the critical size and final coalescence leading to the initiation of a micro-crack. All these stages depend strongly on the material properties and its microstructure as well as on the external conditions like temperature or strain rate. Although the experimental investigation of the ductile failure behavior is quite easy, the numerical simulation of the failure processes requires a precise description of the material plasticity and an exact definition of the failure criterion.
In the recent years many different damage mechanics models for the simulation of ductile failure behavior have been developed. Two groups of models can be distinguished. Models of the first group consider the effect of the accumulated damage in the form of the constitutive equations. The most known model was independently developed by Gurson [1] and Tvergaard and Needleman [2]. The constitutive equation for the yield potential was derived for porous materials. In this equation the void volume fraction was implemented as the damage indicator. Further modifications considered the accelerated process of coalescence after reaching a critical void volume fraction [3]. In the models of the second group critical loading conditions, which led to the failure of material, were introduced. Apart from the equivalent plastic strain, the effect of hydrostatic pressure (stress triaxiality) and Lode angle on the flow potential played an important role. The scientific findings from the last few years show that these both quantities should be considered for the precise description of plasticity, especially of the real materials [4-8].
For the safe design of steel constructions both strength and toughness assessments are usually applied. However, the conventional standards of the strength assessments consider only the local material plasticity, represented by the yield strength. In order to utilize the whole potential of the material capacity strain-based assessments are an alternative to the conventional designing rules [9-10]. The modeling approach presented in this work allows for the description of ductile failure behavior and contributes to the further development of the strain-based concepts.

Damage mechanics model

The model for the simulation of ductile fracture applied in this paper has been derived from the combination of different types of damage approaches. It is based on the formulations given by Bai and Wierzbicki [11], which include the effect of the following two factors: stress triaxiality η (pressure dependence) and the Lode angle Θ (related to the third invariant of the stress deviator) in the constitutive description of the material. The yield potential function proposed by Bai and Wierzbicki is given by Eq. 1.

$$\sigma_{yld} = \sigma(\varepsilon_p) \cdot \left[1 - c_\eta (\eta - \eta_0)\right] \cdot \left[c_\theta^s + \left(c_\theta^{ax} - c_\theta^s\right)\left(\gamma - \frac{\gamma^{m+1}}{m+1} \right) \right] \tag{1}$$

For the estimation of the basic flow curve $\sigma(\varepsilon_p)$ a reference test (for example tensile, upsetting or torsion test) can be chosen arbitrarily, however, the selected test type determines the further procedure for the parameter calibration. This curve is corrected by two terms, which consider the effect of stress triaxiality and Lode angle on the yield potential. The stress triaxiality η is defined as a ratio of hydrostatic pressure to the equivalent stress. The Lode angle θ describes the location of the

yielding point in the deviatoric plane and can be expressed as normalized Lode angle Θ' or as the parameter γ according to Eq. 2-4.

$$\theta = \frac{1}{3}\arccos\left[\frac{\frac{27}{2}\left(\sigma_1 - \frac{\sigma_1+\sigma_2+\sigma_3}{3}\right)\left(\sigma_2 - \frac{\sigma_1+\sigma_2+\sigma_3}{3}\right)\left(\sigma_3 - \frac{\sigma_1+\sigma_2+\sigma_3}{3}\right)}{\left[\frac{1}{2}\left[(\sigma_1-\sigma_2)^2+(\sigma_2-\sigma_3)^2+(\sigma_3-\sigma_1)^2\right]\right]^{\frac{3}{2}}}\right] \tag{2}$$

$$\Theta' = 1 - \frac{6\theta}{\pi} \tag{3}$$

$$\gamma = \frac{\cos\left(\frac{\pi}{6}\right)}{1-\cos\left(\frac{\pi}{6}\right)}\left[\frac{1}{\cos\left(\theta - \frac{\pi}{6}\right)} - 1\right] \tag{4}$$

The yield potential given by Eq. 1 describes the stress state through the stress triaxiality and Lode angle. In order to find the moment when the damage contributes to the failure process, different empirical approaches can be applied. In the models known from the literature [12-16] the strains at the fracture point are usually included in the damage description. The model presented in this paper utilizes the micro-crack initiation as the onset of the damage process. Furthermore, in order to consider the damage-induced softening of a material a damage evolution low based on the energy dissipation is implemented. A damage indicator D characterizes the accumulated damage and reaches a critical D_{cr} value at the final fracture.

Another innovative component of the proposed model is a new definition of the influence of strain rate and temperature on the yield potential. The description of the strain rate impact covers the mechanisms of dislocation slip as well as the dislocation damping, so that this model can be applied to very high strain rates typical for impact loading conditions. The implementation of temperature effect allows for the simulation of Charpy tests at different temperatures. The yield criterion used in the developed model and the definition of D variable are given respectively by Eq. 5 and 6.

$$\begin{aligned}\sigma_{yld} = {} & \left[\sigma(\varepsilon_p)\cdot\left(c_1^{\dot{\varepsilon}}\cdot\ln\dot{\varepsilon}+c_2^{\dot{\varepsilon}}\right)+c_3^{\dot{\varepsilon}}\cdot\dot{\varepsilon}\right]\cdot\left[c_1^T\cdot\exp\left(-c_2^T\cdot T\right)+c_3^T\right]\cdot\left[1-c_\eta(\eta-\eta_0)\right] \\ & \cdot\left[c_\theta^s+\left(c_\theta^{ax}-c_\theta^s\right)\left(\gamma-\frac{\gamma^{m+1}}{m+1}\right)\right]\cdot(1-D)\end{aligned} \tag{5}$$

$$\dot{D} = \begin{cases} 0 & for \quad \varepsilon \le \varepsilon_i \\ \dfrac{\sigma_{yld}\cdot L\cdot\dot{\varepsilon}}{2\cdot G_f} & for \quad \varepsilon_i < \varepsilon < \varepsilon_f \\ D_{cr} & for \quad \varepsilon = \varepsilon_f \end{cases} \tag{6}$$

The symbols used in Eq. 6 have the following meanings: L is the characteristic length of the element; G_f describes the energy needed to open a unit area of a crack and σ_{yld} corresponds to the value of the yield stress at the onset of damage. The damage indicator D starts to play a role in the moment of a micro-crack initiation, when the strain reaches a value ε_i. The final fracture occurs at the strain ε_f.

The description of ductile failure behavior using the presented model requires calibrating of the following parameters:

c_1^{ε}, c_2^{ε}, c_3^{ε} – influence of strain rate,
c_1^{T}, c_2^{T}, c_3^{T} – influence of temperature,
η_0, c_η – influence of stress triaxiality,
c_θ^{s}, m, c_θ^{ax} – influence of Lode angle ($c_\theta^{ax} = c_\theta^{t}$ or c_θ^{c} depending on loading conditions),
D_{cr}, G_f – description of damage evolution.

A detailed description of the particular parameters can be found in [17, 5].

Investigated material

For the study of the ductile failure behavior a reactor pressure vessel steel 22NiMoCr3-7 was utilized. Its chemical composition is given in Table 1. Mechanical properties of this ferritic steel were determined in tensile tests with a smooth bar specimens according to DIN EN 10002; they are listed in Table 2.

Table 1: Chemical composition of steel 22NiMoCr3-7 (mean mass contents in %)

C	**Si**	**Mn**	**P**	**S**	**Cr**	**Mo**
0.20	0.20	0.91	0.005	0.002	0.40	0.49
Ni	**Al**	**Nb**	**Cu**	**Ti**	**V**	**Co**
0.802	0.017	0.002	0.034	0.001	0.005	0.010

Table 2: Mechanical properties of the reactor pressure vessel steel 22NiMoCr3-7

upper yield strength R_{eH} [MPa]	lower yield strength R_{eL} [MPa]	tensile strength R_m [MPa]	uniform elongation A_g [%]	total elongation A_5 [%]
448.5	430.5	582.5	11.2	27.2

Calibration of material parameters and estimation of crack initiation locus

The basic flow curve was estimated in tensile test with smooth bar specimens (reference test) and extrapolated using Hollomon equation. Because the tensile test was chosen as the reference test, the parameters η_0 and C_θ^{t} equal to 0.33 and 1.00, respectively [11]. In the next step the parameters describing the influence of stress triaxiality and Lode angle were calibrated. For this purpose tensile tests with notched round bar and plane strain specimens as well as upsetting tests with notched round bar samples were carried out. The numerical simulation of these results and the comparison of the experimental and numerical simulation results allowed for the estimation of the following parameters: $C_\eta = 0.00$, $C_\theta^{s} = 0.95$, $C_\theta^{c} = 1.00$ and $m = 5.00$. It should be emphasized that for the investigated steel the influence of the hydrostatic pressure on the flow potential is insignificant. Based on these material parameters the crack initiation locus could be estimated.

The ductile crack initiation locus defines the critical strain ε, stress triaxiality η and Lode angle θ at the moment of the crack initiation. The variation of samples geometries leads to the different stress states in the stressed body, so that different sample types are necessary for the proper estimation of this locus. In the present work 3 different notched round bar and 3 notched plane strain specimens were investigated. In order to estimate the initiation of a micro-crack, a direct current potential drop (DCPD) method accompanied the performed tests. This approach is widely used in fracture

mechanics and is based on the change of electrical potential as a consequence of decreasing cross section caused by the presence of a micro-crack. The following numerical simulations of the performed tests allow for the determination of critical values of strain, stress triaxiality and Lode angle at the moment of crack initiation. Based on these results a symmetrical crack initiation locus was calculated using the least squares approach and is presented in Fig. 1.

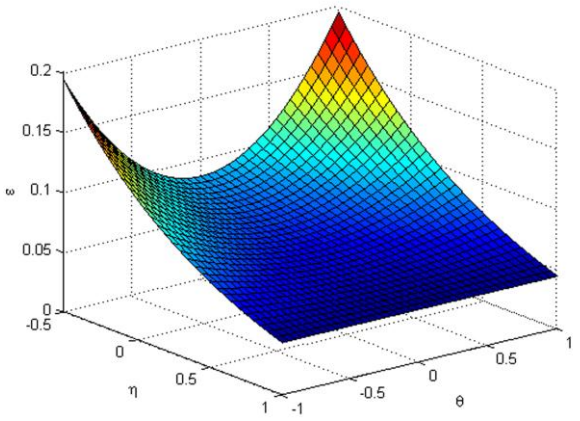

Fig. 1: Crack initiation locus curve for steel 22NiMoCr3-7

The results of the experiments with notched round bar samples were used for the calibration of D and G_f parameters, which describe the damage evolution in the material after initiation of a micro-crack. Fig. 2 shows exemplary force-displacement responses at different steps of parameter calibration for the notched round bar specimen (R=1.5 mm). The simulation curves show clearly the influence of the third invariant of the stress deviator (Lode angle), the crack initiation and damage evolution. The best results were achieved using the above mentioned parameters as well as for D_{cr} = 0,10 and G_f = 300. At the present stage of the model development the parameters, which describe the influence of temperature and strain rate on the yield potential, are being still estimated.

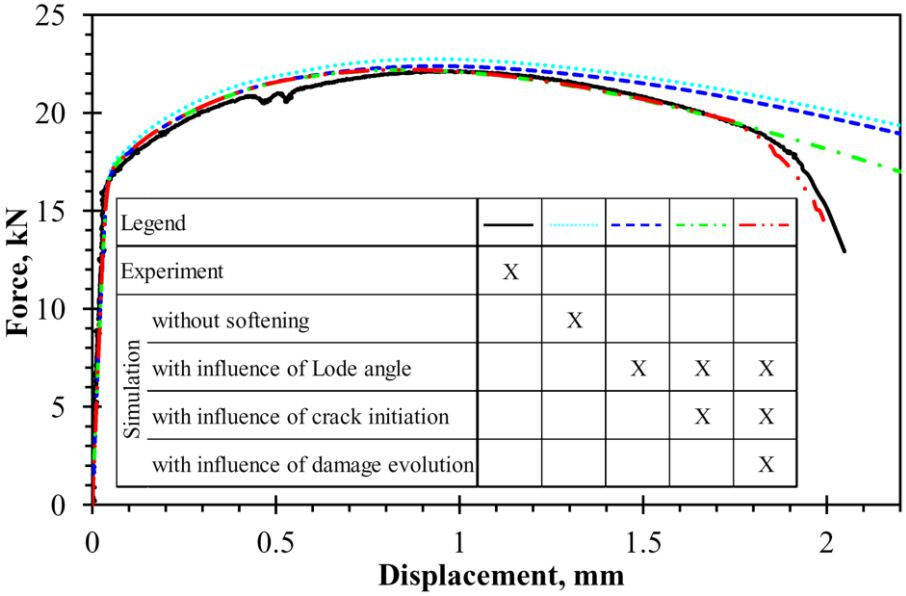

Fig. 2: Force-displacement curves for notched round bar specimen (R=1.5 mm)

Preliminary model validation

The presented model was validated by the simulation of the shear tests and tensile tests with notched plane strain specimens. The first result showed that for the damage indicator $D_{cr} = 0{,}10$ some differences in the estimation of the final fracture between experiment and simulation appeared. For the plane strain samples the final fracture occurred earlier in the experiment than in the simulation. The opposite behavior was observed for the shear samples. This could result from the definition of the damage evolution after crack initiation, which does not consider the influence of the stress state. The simulation and experimental results of the shear test, which was not involved in any parameter calibration, are presented in Fig. 3. The simulation result was obtained for $D_{cr} = 0{,}70$ and shows a good agreement with the experiment.

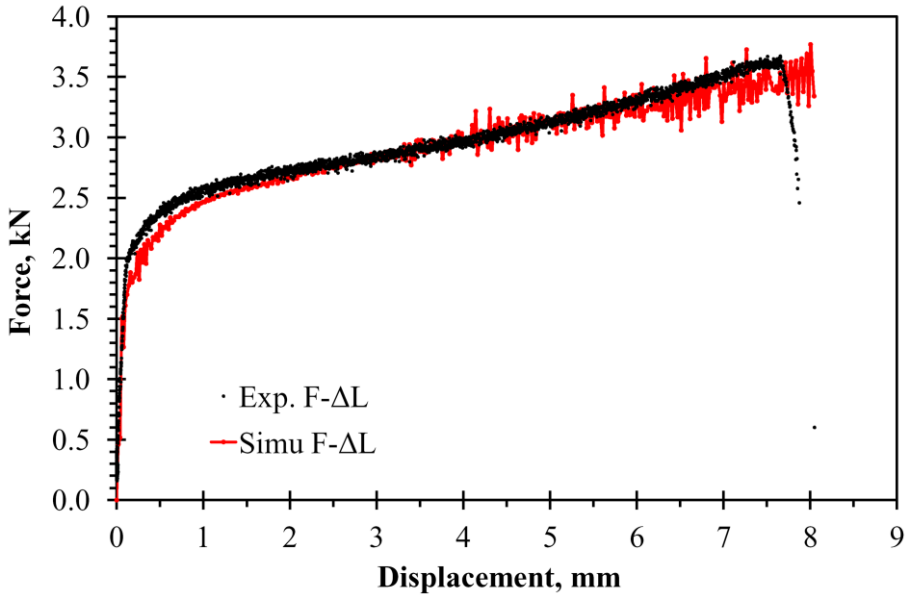

Fig. 3: Experimental and simulation results of the shear test.

Conclusions

The performed scientific work leads to the following conclusions:

- In the presented procedure of the parameter calibration the influence of Lode angle, the crack initiation and damage evolution on the flow potential has been evidenced.
- The flow potential of the investigated material shows extremely small dependence on the hydrostatic pressure.
- Further improvement of the model is focused on redefinition of the damage evolution law in order to achieve better estimation of the final fracture.

References

[1] A.L. Gurson: J. Eng. Mater. Technol.-Trans. ASME Vol. 99(1) (1977), p. 2-15
[2] V. Tvergaard and A. Needleman: Acta Metall. Vol. 32(1) (1984), p. 157-169.

[3] A. Needleman and V. Tvergaard: Int. J. Fract. Vol. 49 (1991), p. 41-67
[4] M. Brunig: Int. J. Plasticity Vol. 15(11) (1999), p. 1237-1264
[5] W.A. Spitzig and O. Richmond: Acta Metall. Vol. 32(3) (1984), p. 457-463
[6] W.A. Spitzig, R.J. Sober and O. Richmond Metall. Mater. Trans. A-Phys. Metall. Mater. Sci. Vol. 7(11) (1976), p. 1703-1710.
[7] X. Gao, G. Zhang, and C. Roe: Int. J. Damage Mech. Vol. 19(1) (2009), p. 75-94
[8] F. Yang, Q. Sun, and W. Hu: Acta Metall. Sinica Vol. 22(2) (2009), p. 123-130
[9] B. Liu, X.J. Liu and H. Zhang: J. Loss. Prev. Process. Ind. Vol. 22 (2000), p. 884-888
[10] E. Østby, C. Thaulow and B. Nythus: Int. J. Press. Vessels Pip. Vol. 84 (1998), p. 337-348
[11] Y.L. Bai and T. Wierzbicki: Int. J. Plasticity Vol. 24(6) (2008), p. 1071-1096
[12] Y. Bao and T. Wierzbicki: J. Eng. Mater. Technol. Vol. 126(3) (2004), p. 314-324
[13] Y. Bao and T. Wierzbicki: Int. J. Mech. Sci. Vol. 46(1) (2004), p. 81-98
[14] M. Dunand and D. Mohr: Int. J. Solids Struct. Vol. 47(9) (2010), p. 1130-1143
[15] J.R. Rice and D.M. Tracey: J. Mech. Phys. Solids Vol. 17(3) (1969), p. 201-217
[16] G.R. Johnson and W.H. Cook: Eng. Fract. Mech. Vol. 21(1) (1985), p. 31-48
[17] J. Lian, M. Sharaf, F. Archie and S. Münstermann: submitted to Int. J. Damage Mech. (2011)